

Particle discrimination in a NaI crystal using the COSINUS remote TES design

G. Angloher,¹ M.R. Bharadwaj,¹ I. Dafinei,^{2,3} N. Di Marco,^{2,4} L. Einfalt,^{5,6}
F. Ferroni,^{3,2} S. Fichtinger,⁵ A. Filipponi,^{7,4} T. Frank,¹ M. Friedl,⁵ A. Fuss,^{5,6} Z. Ge,⁸
M. Heikinheimo,⁹ M. N. Hughes,¹ K. Huitu,⁹ M. Kellermann,¹ R. Maji,^{5,6} M. Mancuso,¹
L. Pagnanini,^{2,4} F. Petricca,¹ S. Pirro,⁴ F. Pröbst,¹ G. Profeta,^{7,4} A. Puiu,^{2,4} F. Reindl,^{5,6}
K. Schäffner,¹ J. Schieck,^{5,6} D. Schmiedmayer,^{5,6} C. Schwertner,^{5,6} M. Stahlberg,^{1,*}
A. Stendahl,⁹ M. Stukel,^{2,4} C. Tresca,^{7,4} F. Wagner,⁵ S. Yue,⁸ V. Zema,^{1,†} and Y. Zhu⁸
(The COSINUS Collaboration)

A. Bento,^{10,1} L. Canonica,¹ and A. Garai¹

¹Max-Planck-Institut für Physik, 80805 München - Germany

²Gran Sasso Science Institute, 67100 L'Aquila - Italy

³INFN - Sezione di Roma, 00185 Roma - Italy

⁴INFN - Laboratori Nazionali del Gran Sasso, 67010 Assergi - Italy

⁵Institut für Hochenergiephysik der Österreichischen Akademie der Wissenschaften, 1050 Wien - Austria

⁶Atominstytut, Technische Universität Wien, 1020 Wien - Austria

⁷Dipartimento di Scienze Fisiche e Chimiche,

Università degli Studi dell'Aquila, 67100 L'Aquila - Italy

⁸SICCAS - Shanghai Institute of Ceramics, Shanghai - P.R.China 200050

⁹Helsinki Institute of Physics, Univ. of Helsinki, 00014 Helsinki - Finland

¹⁰LIBPhys-UC, Physics Departments, University of Coimbra, 3004-516 Coimbra - Portugal

(Dated: July 21, 2023)

The COSINUS direct dark matter experiment situated at Laboratori Nazionali del Gran Sasso in Italy is set to investigate the nature of the annually modulating signal detected by the DAMA/LIBRA experiment. COSINUS has already demonstrated that sodium iodide crystals can be operated at mK temperature as cryogenic scintillating calorimeters using transition edge sensors, despite the complication of handling a hygroscopic and low melting point material. With results from a new COSINUS prototype, we show that particle discrimination on an event-by-event basis in NaI is feasible using the dual-channel readout of both phonons and scintillation light. The detector was mounted in the novel *remoTES* design and operated in an above-ground facility for 9.06 g·d of exposure. With a 3.7 g NaI crystal, e^-/γ events could be clearly distinguished from nuclear recoils down to the nuclear recoil energy threshold of 15 keV.

I. INTRODUCTION

In the field of direct dark matter searches null-results have been reported by most experiments [1] with the notable exception of DAMA/LIBRA [2]. DAMA/LIBRA measures scintillation light created by particle interactions in NaI target crystals at room temperature. An annual modulation of the recorded event rate has been observed for many years, which is consistent with dark matter particle interactions, but incompatible with results from other direct searches in this interpretation [1]. The origin of the signal remains unclear. Several experiments have set out to study this phenomenon using the same target material, and strong constraints on

the modulation amplitude have been reported by COSINE-100 [3] and ANAIS [4], which follow a similar detection principle as DAMA/LIBRA. Among the NaI experiments, COSINUS (Cryogenic Observatory for Signals seen in Next generation Underground Searches) will be the only one to feature a direct measurement of the nuclear recoil energy per event. This is possible through the use of transition edge sensors (TES) which are coupled to the NaI target crystals to provide another channel in addition to the scintillation light. NaI poses certain difficulties when operated in this calorimetric approach, such as hygroscopicity and a low melting point [5]. A solution to this problem is the *remoTES* design, where the TES sensor is deposited on a separate wafer, which is then coupled to the absorber crystal using an Au-wire and pad [6]. The first results of this coupling scheme for detectors with Si and TeO₂ absorbers were described

* Corresponding author, martin.stahlberg@mpp.mpg.de

† Corresponding author, vanessa.zema@mpp.mpg.de

in Ref. [6]. We demonstrate in this work that the same principle is applicable to NaI crystals, and present results from the first NaI-remoTES detector. In particular, we show that discrimination between e^-/γ events and nuclear recoils on an event-by-event basis is possible in NaI, which constitutes a milestone for COSINUS.

II. DETECTOR MODULE

The detector module consists of a remoTES phonon detector (cf. [6]) shown in Fig. 1 and 2a and a silicon-on-sapphire (SOS) wafer as light detector (cf. Fig. 3). The absorber is a $(10\times 10\times 10)\text{ mm}^3$ NaI-crystal with a mass of 3.7 g, manufactured by the Shanghai Institute of Ceramics (SICCAS). An Au-foil, cut from an ingot to a thickness of $1\text{ }\mu\text{m}$ and an area of 4 mm^2 , was glued on the absorber with EPO-TEK 301-2, a two component low out-gassing epoxy resin [7]. The residual resistivity ratio (RRR) of the Au-foil is about 22. The Au-foil was coupled to the TES wafer with two Au-wire bonds with a diameter of $17\text{ }\mu\text{m}$ each and lengths of 6.7 mm and 10.3 mm. A zoomed picture of the remoTES coupling to the absorber is shown in Fig. 2b. An ohmic heater, fabricated on a $(3\times 3)\text{ mm}^2$ silicon pad with a thickness of 1 mm, was glued with EPO-TEK 301-2 on the surface of the NaI-absorber, and was used to inject heater pulses into the crystal. A ^{55}Fe X-ray source with an activity of 3 mBq was taped to the copper holder facing the NaI-absorber, and irradiated it from the side as indicated in Fig. 2a. The wafer is a $(10\times 20\times 1)\text{ mm}^3$ Al_2O_3 crystal, with an evaporated W-TES of $(100\times 407)\text{ }\mu\text{m}^2$ in area and a thickness of 156 nm with two aluminum bonding pads for the connection to the bias circuit. The Au-wires from the Au-foil are bonded on the Au-bridge which overlaps with the W-film (see Fig. 1). Another Au-stripe is used as a thermal link connecting the TES to the thermal bath; its resistance is about $82.3\text{ }\Omega$ at room temperature. An Au-film with an area of $(200\times 150)\text{ }\mu\text{m}^2$ and a thickness of 100 nm, deposited on the wafer surface, is used to inject heater pulses and thus monitor the temperature of the TES.

The light detector is a $(20\times 20\times 0.4)\text{ mm}^3$ SOS wafer, equipped with a $(284\times 423)\text{ }\mu\text{m}^2$ W-TES of 200 nm thickness, which has two $(526\times 1027)\text{ }\mu\text{m}^2$ phonon collectors (Al/W bilayers) of $1\text{ }\mu\text{m}$ thickness [8]. It is mounted on the lid of the copper holder, which is used to protect the NaI from humid air. The light detector is irradiated with a second ^{55}Fe calibration source of similar activity as the one shining on the absorber. A picture of the light de-

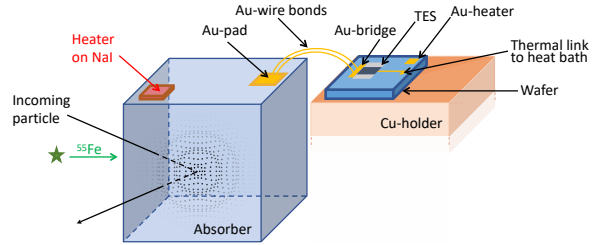


FIG. 1: Schematic of the remoTES detector. The TES is deposited on a wafer, which is separated from the absorber crystal. The coupling between the absorber and the TES consists of an Au-pad glued on the absorber surface and connected to the TES by two Au-wire bonds [6].

tor (Fig. 3a) and an enlarged view of the wire bonding of its TES (Fig. 3b) are shown in Fig. 3. In the following, we refer to the NaI-remoTES as the phonon channel and the light detector as the light channel, interchangeably. The description of the detector components is summarised in Tab. I.

Component	Dimension
NaI-absorber	$(10\times 10\times 10)\text{ mm}^3$
Au-pad on NaI	Area: 4 mm^2 Thickness: $1\text{ }\mu\text{m}$ Glue: EPO-TEK 301-2 RRR: ≈ 22
Two Au-wires	Lengths: (6.7, 10.3) mm Diameter: $17\text{ }\mu\text{m}$
Al_2O_3 wafer	$(10\times 20\times 1)\text{ mm}^3$
W-TES on wafer	Area: $(100\times 400)\text{ }\mu\text{m}^2$ Thickness: 156 nm Area heater: $(200\times 150)\text{ }\mu\text{m}^2$ Thickness heater: 100 nm
SOS wafer	$(20\times 20\times 0.4)\text{ mm}^3$
W-TES on SOS wafer	Area: $(300\times 450)\text{ }\mu\text{m}^2$ Thickness: 200 nm

TABLE I: Dimensions of all components of phonon detector and light detector.

III. DATA TAKING

The measurement was carried out in an above-ground wet dilution refrigerator at the Max Planck Institute for Physics in Munich. The cryostat is equipped with four superconducting quantum interference devices (SQUIDs) from the APS company [9] and continuously read out with a 16-bit analog-digital converter at a sampling frequency

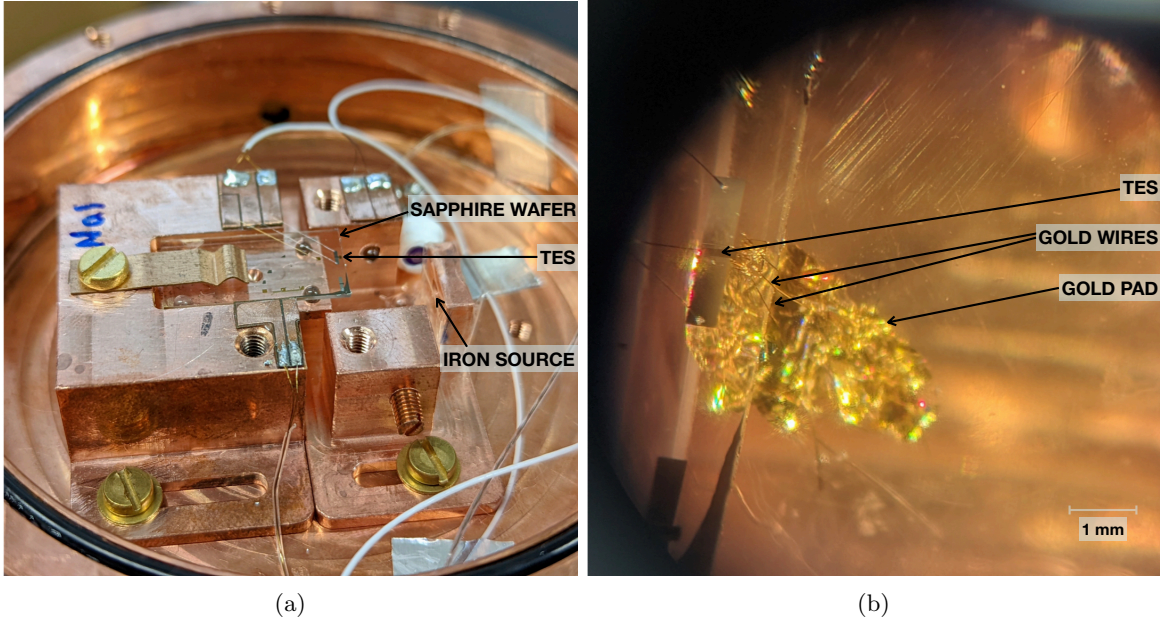


FIG. 2: (a) The remoTES wafer mounted in the copper holder. The sapphire wafer is placed on sapphire balls and held by a bronze clamp. A ^{55}Fe source is taped on a copper piece facing the absorber for the purpose of energy calibration. (b) Microscopic view of the Au-pad glued on the NaI-crystal and the wire bonding to the remoTES.

of 50 kS/s. To reduce the background event rate induced by cosmic and ambient radiation, a lead wall with a thickness of 10 cm was built around the refrigerator. Three subsequent datasets were recorded and are discussed in this work: a background dataset with only the (module-internal) ^{55}Fe sources present, a ^{57}Co calibration dataset, and an additional neutron calibration dataset using an AmBe source. The duration and effective exposure of each dataset are given in Table II.

IV. DATA ANALYSIS

For the three datasets discussed above, the continuous stream from the phonon channel is triggered in software using an optimal filter trigger (cf. Ref. [10] and Ref. [11]). The light channel is read out in parallel. The filter is created from a parametric description of the NaI channel pulse shape based on Ref. [12] and a noise power spectrum obtained from randomly drawn empty noise traces. The typical pulse shape of absorber recoils for the NaI channel is shown in Fig. 4a and features a very long decay time. A baseline energy resolution of the phonon channel of 2.07 ± 0.06 keV is determined by superimposing the pulse shape onto a set of ran-

domly drawn empty baselines and reconstructing these artificial events. The resulting amplitude distribution is illustrated in Fig. 4b. The baseline resolution of the SOS light detector was determined to be 2.02 ± 0.05 keV_{ee} (electron-equivalent) using the same technique.

The datasets were triggered with a threshold of 10 keV, where no noise triggers were observed. The energy scale for the aforementioned results comes from a fit to the peaks visible in the ^{57}Co dataset; this is illustrated in Fig. 5. Peaks from the ^{55}Fe source could not be observed, as their energies of 5.9 keV and 6.4 keV are below the energy threshold. The optimum filter amplitude is used as an energy estimator. In the energy range from threshold up to ~ 500 keV, the detector response is in good approximation linear. All datasets were cleaned by applying a set of quality cuts. Severely unstable detector operation intervals are removed by monitoring the reconstructed amplitude of injected heater pulses over time. Single voltage spike events are removed by cutting on the ratio of the numerical derivative of the pulse to the baseline RMS. The RMS from the optimal filter reconstruction and the RMS from an additional truncated standard event fit reconstruction (cf. e.g. Ref. [13]) are used to remove pile-up events and events from particle in-

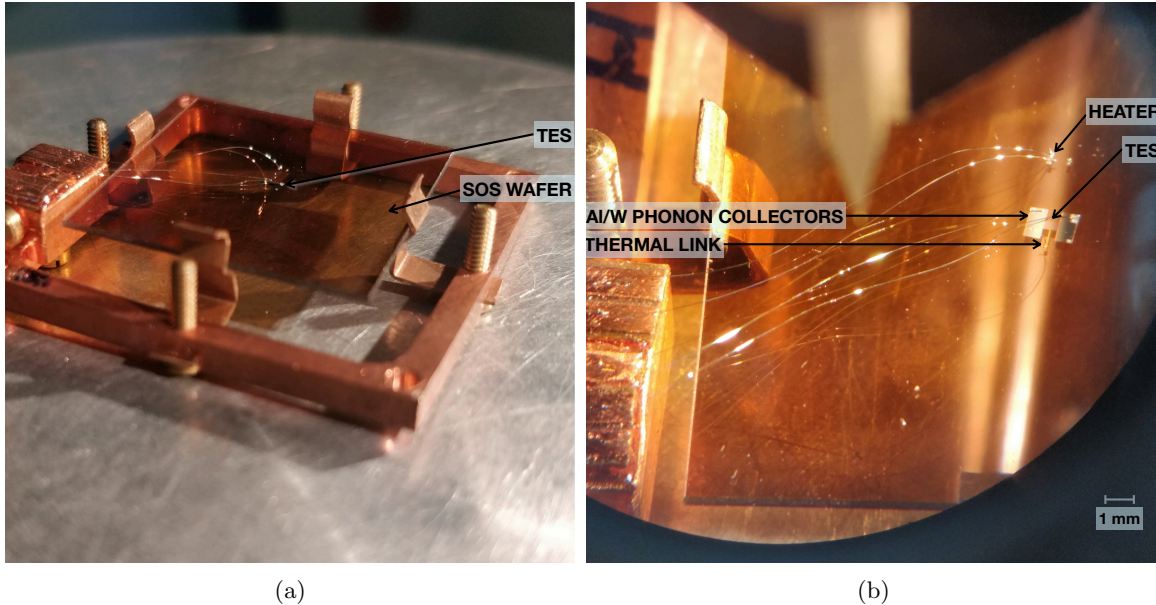


FIG. 3: (a) SOS light detector mounted in a copper holder. (b) Microscopic view of the electrical connections of the light detector TES and of its separate ohmic heater.

Measuring time (h)	Calibration sources	Event rate (cps)	Exposure (g·d)
17.73	^{57}Co	0.57	2.73
16.40	AmBe	0.62	2.53
24.61	(none)	0.37	3.79

TABLE II: Measuring times, exposures, event rates and calibration sources for the three datasets.

teractions in the sapphire wafer. The effect of each quality cut is assessed by simulating pulses with a flat energy spectrum on the set of randomly drawn detector baselines and studying the fraction of surviving events as a function of the simulated energy. We find that the detector threshold of 10 keV is only nominal, i.e. no simulated signal event survives down to this energy. This is due to varying noise conditions in the above-ground setup, very long pulse decay time, and the presence of particle recoils in the wafer, which require strong quality cuts to be discarded. An analysis threshold of 15 keV is used in the following, where the signal survival probability is still about 5%. Above this threshold, no wafer-induced events or noise events are observed in the background dataset.

V. DISCRIMINATION OF NUCLEAR RECOIL BANDS

The light yield (LY) is defined as the ratio of the energy measured in the light channel and the

energy measured in the phonon channel for each event. It enables the discrimination of different recoil event classes. In Fig. 6 the LY is shown as a function of the phonon channel energy for the background and the neutron calibration datasets, respectively. We use a parametrization of the recoil bands and of the spectra which contribute to them, described in detail in [14]. For events in the electron band, the LY is normalized to 1. Two quenched bands are expected for Na and I nuclear recoils due to the different masses of the nuclei. We observe that these cannot be reliably separated by the likelihood fit, which yields a high correlation between parameters for the two bands. Therefore, we conservatively estimate the parameters of the e^-/γ band from the background dataset, and compare them to the observed events in the neutron calibration dataset. We will address a modification of the band description and separation of the individual nuclear recoil bands in a future publication. Figure 6 shows the result of the likelihood bandfit to the background dataset (left panel) and to the neutron calibration

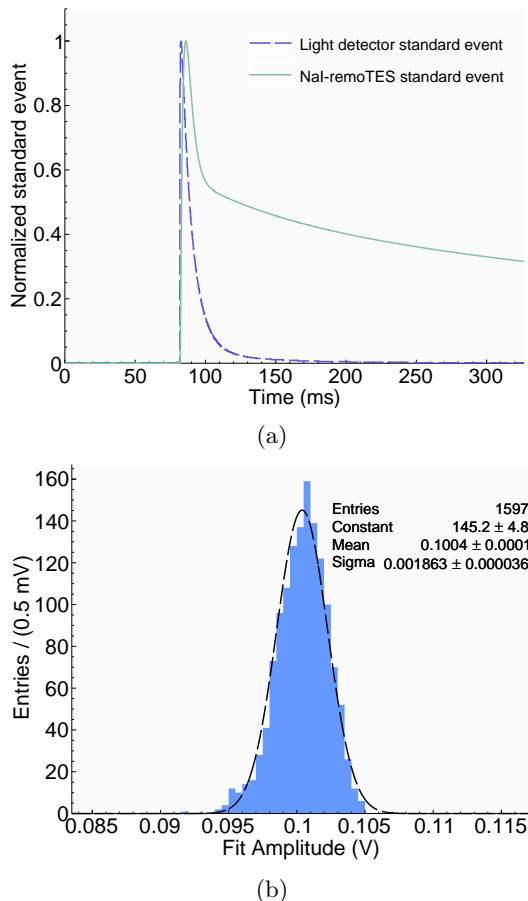


FIG. 4: (a) Normalized standard events in the light detector (dashed, dark-blue curve) and in the NaI-remoTES detector (solid, water-green curve).

(b) Reconstructed pulse height (truncated fit) distribution for artificial pulses, which are obtained by superimposing an averaged signal pulse onto empty traces for the phonon channel.

dataset (right panel), using 90% boundaries for the e^-/γ band. It can be clearly seen that a new population of events appears below the e^-/γ band, far outside the 2σ boundary. The additional band is quenched in LY to ~ 0.5 at energies above 100 keV, and the LY appears to be decreasing as the recoil energy approaches the threshold. In Ref. [15], a similar decline of the quenching factor

in NaI at lower energies was reported for measurements at room temperature and with Tl-doped crystals. Above ca. 100 keV, the quenching factor observed with our prototype is even higher than in Ref. [15]. At increasing energy, a downward tilt of the e^-/γ band is visible, which is due to increasing nonlinearity in the light detector response.

VI. CONCLUSIONS

This measurement marks the first proof of event-by-event particle discrimination in a cryogenic NaI detector. We operated a COSINUS prototype with a remoTES sensor, which displayed a baseline resolution of 2 keV despite suboptimal, above-ground conditions. It was calibrated with a ^{57}Co γ source and analysed with a nuclear recoil threshold of 15 keV. Particle discrimination was verified with neutrons from an AmBe source. In Ref. [6], the remoTES design was suggested as an improved read-out for delicate absorber materials, which are for example hygroscopic or feature a low melting point. This work shows that the design is indeed suitable for NaI absorbers. The next step in the COSINUS detector optimization strategy in the direction of achieving an energy threshold of 1 keV is an underground measurement with a similar detector, in order to assess its performance in a low-background environment. This measurement has already been performed, and will be subject of a future publication.

ACKNOWLEDGMENTS

This measurement was possible thanks to the use of the CRESST cryogenic facility and detector production infrastructure at the Max Planck Institute for Physics (MPP). Similarly, the support from the MPP mechanical workshop was invaluable. We thank SICCAS for producing the NaI crystal employed in this measurement. This work has been supported by the Austrian Science Fund FWF, stand-alone project AnaCONDa [P 33026-N]. This project was supported by the Austrian Research Promotion Agency (FFG), project ML4CPD.

[1] J. Billard et al. Direct detection of dark matter—APPEC committee report. *Reports on Progress in Physics*, 85(5):056201, 2022. doi:

10.1088/1361-6633/ac5754.
[2] R. Bernabei et al. Recent results from DAMA/LIBRA and comparisons. *Moscow Uni-*

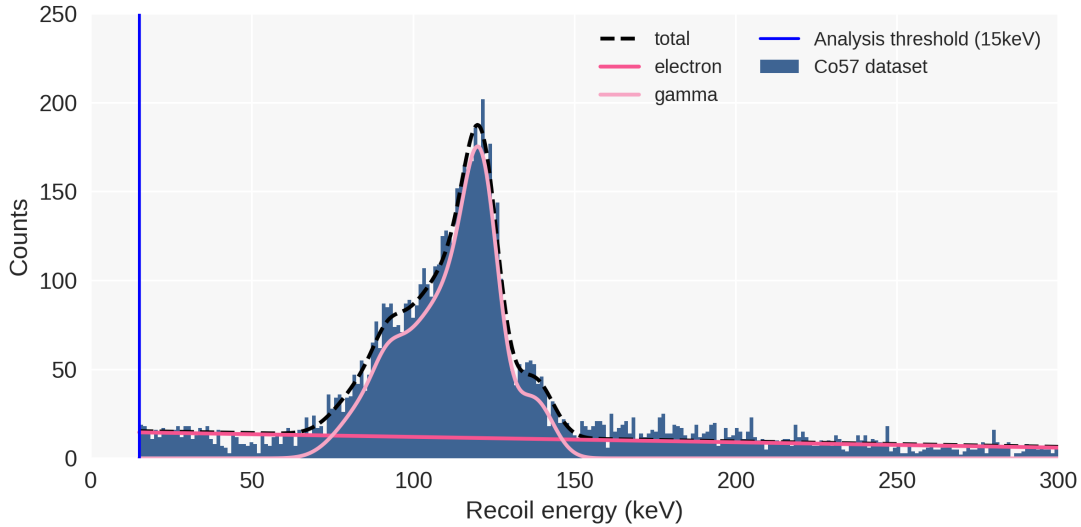


FIG. 5: Energy spectrum from the ^{57}Co γ calibration measurement. Different components are fitted using a parametric description. The fit includes gaussian peaks at 136 keV and 122 keV on top of a linearly decreasing background, as well as a γ escape peak due to I K- α , expected at around 89 keV. The parametric fit also considers ‘shoulders’ on the left side of each peak, which originate from ^{57}Co γ s depositing a fraction of their energy in parts of the setup before reaching the detector.

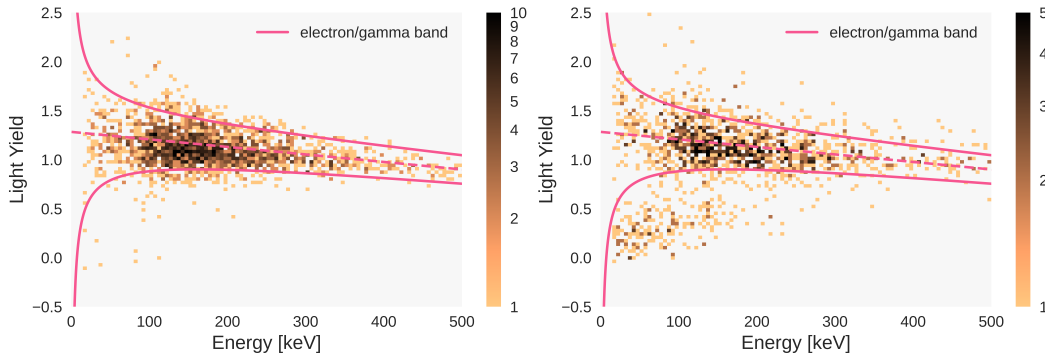


FIG. 6: 2D histograms of LY versus phonon channel energy with color-coded number of entries. Left: background dataset with parametric description of the e^-/γ band obtained from the log-likelihood fit. Right: same plot for the AmBe neutron calibration dataset. A second population of events is visible below the e^-/γ band.

versity Physics Bulletin, 77(2):291–300, 2022. doi: 10.15407/jnpae2021.04.329.

- [3] G. Adhikari et al. Three-year annual modulation search with COSINE-100. *Physical Review D*, 106(5):052005, 2022.
- [4] J. Amaré et al. Dark matter annual modulation with ANAIS-112: Three years results. *Moscow University Physics Bulletin*, 77(2):322–326, 2022.
- [5] G. Angloher et al. Results from the first cryogenic NaI detector for the COSINUS project. *Journal of Instrumentation*, 12(11):P11007, 2017. doi: 10.1088/1748-0221/12/11/P11007.

- [6] G. Angloher et al. First measurements of re-moTES cryogenic calorimeters: Easy-to-fabricate particle detectors for a wide choice of target materials. *Nuclear Instruments and Methods in Physics Research Section A: Accelerators, Spectrometers, Detectors and Associated Equipment*. doi:10.1016/j.nima.2022.167532.

[7] Note1. <https://www.epotek.com/>.

- [8] G. Angloher et al. Limits on WIMP dark matter using scintillating CaWO_4 cryogenic detectors with active background suppression. *Astropart. Phys.*, 23:325–339, 2005. doi:

- 10.1016/j.astropartphys.2005.01.006.
- [9] Applied Physics Systems. <https://appliedphysics.com/>.
- [10] E. Gatti and P. F. Manfredi. Processing the signals from solid-state detectors in elementary-particle physics. *Riv. Nuovo Cim.*, 9(1):1–146, Jan. 1986. ISSN 1826-9850. doi:10.1007/BF02822156.
- [11] G. Angloher et al. Results on MeV-scale dark matter from a gram-scale cryogenic calorimeter operated above ground. *Eur. Phys. J. C*, 77(9): 637, Sept. 2017. ISSN 1434-6044, 1434-6052. doi: 10.1140/epjc/s10052-017-5223-9.
- [12] F. Pröbst et al. Model for cryogenic particle detectors with superconducting phase transition thermometers. *Journal of low temperature physics*, 100: 69–104, 1995. doi:10.1007/BF00753837.
- [13] G. Angloher et al. Commissioning run of the CRESST-II dark matter search. *Astroparticle Physics*, 31(4):270–276, 2009. doi: 10.1016/j.astropartphys.2009.02.007.
- [14] G. Angloher et al. Testing spin-dependent dark matter interactions with lithium aluminate targets in CRESST-III. *Physical Review D*, 106(9):092008, 2022. doi:10.1103/PhysRevD.106.092008.
- [15] D. Cintas et al. Quenching Factor consistency across several NaI (Tl) crystals. In *Journal of Physics: Conference Series*, volume 2156, page 012065. IOP Publishing, 2021. doi:10.1088/1742-6596/2156/1/012065.